MATERIALS PHYSICS AND MECHANICS RESEARCH ARTICLE

Submitted: July 30, 2025 **Revised: August 28, 2025** **Accepted: October , 2025**

Structural response of reinforced, steel fiber reinforced and prestressed geopolymer concrete beams subjected to transverse loading

T.Q.K. Lam [1] ✉, K.S. Sreekeshava [2], S. Kumar [3], C. Bhargavi [2], B.N. Skanda Kumar [2], G. Gayathri [2], Y.R. Suresh [2]

[1] Faculty of Civil Engineering, Mien Tay Construction University, Vinh Long, Vietnam

[2] Jyothy Institute of Technology, Affiliated to Visveswaraya Technological University, Belagavi, India

[3] Bureau veritas, Bangalore, India

✉ lamkhai@mtu.edu.vn

ABSTRACT

The workability of the geopolymer concrete mixes was evaluated in accordance with prevailing code of practice. Furthermore, regression analysis was carried out to establish correlations among the strength properties. Fly ash was considered as the primary binder, activated with NaOH and Na_2SiO_3 solutions. The beam mixes were selected based on trial combinations that achieved the highest compressive strength of 41.63 MPa at a water-fly ash ratio of 0.23. To investigate the structural performance, beams of generally reinforced, steel fiber reinforced and prestressed geopolymer concrete with comparable geometries were fabricated and tested under two-point loading. The results revealed that steel fiber reinforced and prestressed geopolymer concrete beams exhibited 14 and 32 % higher ultimate strength, respectively, as compared with generally reinforced geopolymer concrete beams. Moreover, beam stiffness improved by 22 % (steel fiber reinforced geopolymer concrete) and 25 % (prestressed geopolymer concrete). All the beam types satisfied serviceability limits, with deflections below the code-specified span/250 ratio at cracking load. Strain measurements indicated reductions of 10 % in steel fiber reinforced geopolymer concrete and 40 % in prestressed geopolymer concrete relative to generally reinforced geopolymer concrete, with maximum strains of 0.036 (steel fiber reinforced geopolymer concrete), 0.035 (prestressed geopolymer concrete) and 0.030 (generally reinforced geopolymer concrete). Ductility ratios were observed to improve by 6–7 % in both steel fiber reinforced geopolymer concrete and prestressed geopolymer concrete beams. Crack analysis revealed that the flexural failures were predominant in generally reinforced and steel fiber reinforced geopolymer concrete beams, while prestressed geopolymer concrete beams exhibited shear-dominated failures with diagonal tension cracks.

KEYWORDS

stiffness • geopolymer • deflection • polymerization • alkalinity

Citation: Lam TQK, Sreekeshava KS, Kumar S, Bhargavi C, Skanda Kumar BN, Gayathri G, Suresh YR. Structural response of reinforced, steel fiber reinforced and prestressed geopolymer concrete beams subjected to transverse loading. *Materials Physics and Mechanics*. 2025;53(5): 150–163.
http://dx.doi.org/10.18149/MPM.5352025_13

Introduction

The geopolymer concrete (GPC) is produced by blending geopolymer binders with certain aggregates. These binders are formed by chemically activating aluminosilicate rich-source materials using alkaline solutions. This leads to formation of polymeric structures with characteristics comparable to natural rocks [1]. Owing to their superior durability,

fire resistance, mechanical strength and strong adhesion between the aggregates and steel reinforcement, these binders have emerged as sustainable alternative to ordinary Portland cement (OPC) [2]. The increasing interest in GPC is attributed to its nature friendly properties, having potential to reduce carbon emissions, while delivering high performance structural properties [3].

Multiple industrial by-products such as fly-ash, silica fume, ground granulated blast furnace slag (GGBS), metakaolin, sawdust and rice husk ash have been considered as precursors in synthesis of geopolymers [4]. These source materials can be used individually or in combination, with mix proportions. The proportions are often selected through trial optimisation or based on past experimental evidence to meet structural performance requirements.

In this investigation, fly ash has been employed as primary binder, activated with a 14M NaOH solution and Na_2SiO_3 solution in the ratio of 1:2.5. Manufactured sand (M-sand) and crushed stone (10–12 mm) served as fine and coarse aggregates respectively. A polycarboxylate-based superplasticiser (Glenium 220R, BASF) was used at 2 % by weight of the binder to ensure adequate workability. It shall be not4ed that previous studies have shown that workability and strength of GPC are governed by water-geopolymer solid ratio, with strength generally increasing at lower water content [5,6]. Full strength maturity of GPC is typically achieved through thermal curing for 24 h at 65–70 °C [7].

The strength relationships of GPC are mostly compared with established standards for conventional concrete. For compressive-tensile correlations, ACI-318-08 [8] proposes $f_t = 0.59\sqrt{f_{ck}}$, while CIB-FIB [9] and Neville [10] suggest $f_t = 0.30\sqrt{f_{ck}}$ and $f_t = 0.23\sqrt{f_{ck}}$, respectively. Similarly for compressive-flexural correlations, IS 456-2000 [11], Aci-318 and BS 8110 [12] provide relationships such as $f_r = 0.70\sqrt{f_{ck}}$, $f_r = 0.62\sqrt{f_{ck}}$ and $f_r = 0.60\sqrt{f_{ck}}$. Although such empirical expressions exist for OPC-based systems, equivalent validated models for GPC-mainly when modified with fibers-remain limited.

Steel fibers, when randomly distributed in the matrix, arrest crack propagation and improve both post-cracking strength and ductility [13]. Research works have shown that, while the inclusion of fibers may moderately affect compressive strength with variations of about 3 at 0.25 % fiber content and 8 at 1 % [14], it significantly enhances flexural and tensile performance [15–17]. The load bearing capacity after cracking increases due to the bridging action of fibers, which alters the failure mechanism from brittle to ductile [18]. It must as well be noted that incorporating steel fibers reduces the workability of fresh concrete, necessitating optimisation of fiber volume based on trial data [19–22]. Correlation models for fiber-reinforced OPC concrete have as well been proposed [23–25], but their direct applicability to fiber reinforced GPC has not been comprehensively validated.

Although previous studies confirm the potential of GPC as a sustainable alternative to OPC and list out the beneficial role of steel fibers in improving tensile and flexural behaviour, limited research has been done on the comparative structural performance of generally reinforced (GR-GPC), steel fiber reinforced (SFR-GPC) and prestressed GPC (PS-GPC) beams under flexural loading. Further, the development of reliable correlation models to evaluate the strength parameters of fiber-reinforced GPC is still in its early stages. These gaps restrict the wider applications of GPC in structural members

requiring high ductility, stiffness and load carrying efficiency. This study hence aims to investigate and compare the mechanical and flexural performance of GR-GPC, SFR-GPC and PS-GPC beams and establish their suitability for structural applications.

Materials and Methods

Geopolymer concrete mixtures were prepared by varying the percentage of fly-ash as the primary binder. The workability of each mixture was evaluated in accordance with the relevant code of practice. Regression analysis was performed to establish correlation among the strength parameters. The mixture that achieved the maximum compressive strength was selected for fabrication of generally reinforced beams.

To study the effects of fiber, steel fiber reinforced GPC mixtures (SFR-GPC-M) were prepared by incorporating barying fiber volume fractions (0.5, 1 and 1.5 %) into the optimised GPC mixture. The SFR-GPC mixture that demonstrated the best performance in terms of compressive, tensile and flexural strength was chosen for beam casting. Prestressed beams (PS-GPC) and generally reinforced beams (GR-GPC) were also fabricated using optimised GPC-M.

To ensure a statistical reliability and minimise experimental error, three beams were cast and tested in each category (GR-GPC, SFR-GPC and PS-GPC). The sample size of three was chosen in line with common practice in structural experimental studies, where triplicate specimen provide sufficient reproducibility and allow for identification of outliers. All the beams were of identical dimensions, enabling direct comparisons.

The beams were subjected to a four-point bending test to examine flexural performance. Structural parameters such as cracking load, ultimate load, stiffness, ductility, strain distribution and crack pattens were recorded and analysed.

Basic material testing

The source material employed in this study was Class F fly ash sourced from Raichur Thermal Power Corporation Limited (RTPCL), Karnataka, India. The fly ash confirmed to IS 3812 2003 (part 1&2) [26]. Its chemical and physical properties are presented in Table 1. The scanning electron microscopy (SEM) image of the fly ash shown in Fig. 1.

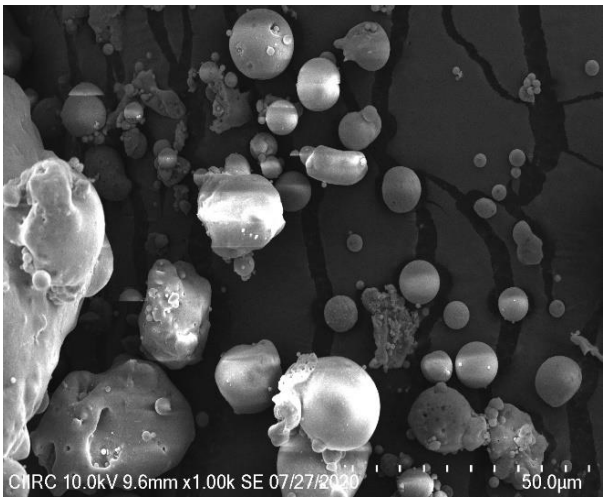

Fig. 1. Scanning electron microscopy image of fly ash (5000 Magnification)

Table 1. Attributes of fly ash

Sr. No	Details	Attributes
1	Relative density	2.08
2	Blain's air permeability, m^2/kg	329.00
3	Silicon Di Oxide (SiO_2), wt. %	63.01
4	Aluminium Oxide (Al_2O_3), wt. %	31.60
5	$SiO_2 + Al_2O_3 + Fe_2O_3$, wt. %	94.61

Laboratory grade sodium hydroxide (NaOH) flakes are used to prepare the alkaline solution. The physical and chemical properties are shown in Table 2. Alkaline liquid preparation involved the utilization of laboratory-grade sodium silicate (Na_2SiO_3). Its properties are summarized in Table 3. Steel fibers were produced from regular drawn steel wires cut into lengths. Their properties are given in Table 4.

Table 2. Attributes of sodium hydroxide

Sr. No	Description	Attributes
1	Appearance	Flake
2	Specific gravity	1.39
3	Sodium hydroxide, wt. %	97.4
4	Sodium carbonate, wt. %	1.6

Table 3. Attributes of sodium silicate

Sr. No	Description	Attributes
1	Flow	Viscous
2	Specific gravity	1.35
3	SiO_2, wt. %	58.25
4	Mg_2O, wt. %	8.10
5	Water content, wt. %	32.80

Table 4. Attributes of steel fibre

Sr. No	Description	Attributes
1	Dimensions, mm^2	36.00 × 0.60
2	Relative density	7.85
3	Elastic Modulus, GPa	200.00
4	Aspect ratio	60.00

A high-performance superplasticizers based on polycarboxylic ethers, marketed under the trade name Glenium 220R (BASF Construction Chemicals), was used in the trial mixes. The admixture confirms to IS 9103:1999 [27]. For improved workability, a dosageof 1–2 % by mass of fly ash was adopted.

Mix proportion and preparation of concrete

The density of GPC varies between 2350 to 2460 kN/m^3 [28]. Trial concrete mixes were formulated by adjusting the percentage of fly ash while maintaining a constant concrete density. The alkaline activator solution consisted of 14 M NaOH and Na_2SiO_3 prepared one day prior to mixing with fixed water content of 130 L/m^3 [29]. To maintain stability, the prepared NaOH solution was stored in air-tight, high-density polyethylene containers at room temperatures. This prevented carbonation and ensured consistency in molarity.

A polycarboxylate ether-based superplasticizer Glenium 220R was added in the range of 1–2 % by mass of fly ash to improve the workability. The mix proportions are presented in Table 5. Figure 2 presents the methodology of preparation and curing of GPC specimen including their casting, specimen after 24 h of setting and specimen arranged inside hot air curing chamber (HACC) for thermal c using at 65 °C for 24 h.

(a) (b) (c)

Fig. 2. Preparation and curing of geopolymer concrete specimens: (a) casting process showing the placement of fresh GPC into moulds in layers followed by compaction; (b) demoulded cube, cylinder, and prism specimens after 24 h of setting; (c) specimens arranged inside the hot air curing chamber (HACC) for thermal curing at 65 ºC for 24 h

Table 5. Mix proportions

Trials	Percentage of fly ash	*FA*, kg/m^3	*ca*, kg/m^3	*fa*, kg/m^3	NaOH, kg/m^3	Na_2SiO_3, kg/m^3	Water to fly ash ratio
GPC-M_1	15.5	314.6	991.72	779.03	89.82	224.4	0.41
GPC-M_2	17.2	356.58	968.4	760.6	89.82	224.41	0.36
GPC-M_3	19.1	398.29	944.08	742.7	89.82	224.4	0.32
GPC-M_4	21.3	439.03	921.4	721.8	89.82	224.4	0.29
GPC-M_5	23.1	479.83	898.6	704.66	89.82	224.4	0.27
GPC-M_6	25.2	522.42	873.12	682.2	89.82	224.4	0.24
GPC-M_7	27	563.16	851.56	667.4	89.82	224.4	0.23
GPC-M_8	29.3	606.57	828	650.59	89.82	224.4	0.21
GPC-M_9	30.9	645.48	804.4	636.3	89.82	224.4	0.18
FA is fly ash, ca is coarse aggregates, fa is fine aggregates							

Casting and curing of GPC

The fresh concrete mixtures as indicated in above Table 5 were poured into moulds following the mixing process. Cylindrical and cube specimens were formed in three layers, while prismatic specimens were formed in two layers. Each layer was compacted by applying manual strokes with a tamping bar and vibration on a vibrating table for 15 to 20 sec.

Following the casting process, the test specimens were covered with a polyethylene sheet, as illustrated in Fig. 2, in order to reduce water evaporation. For a period of 7 days, the specimen was allowed to rest [30]. Following a resting period, all specimens underwent temperature curing in a hot air curing chamber (HACC), as depicted in Fig. 2. Details regarding the arrangement, construction, performance, and technical specifications

of the HACC are elaborated elsewhere [31]. Curing of all specimens was conducted at 65 °C for a duration of 24 h [32]. Subsequently, the specimens were cooled at room temperature for 20 to 24 h prior to testing.

Mechanical strength of hardened concrete

The compressive, split tensile and flexural strengths of hardenend geopolymer concrete mixtures are summarized in Table 6 and further illustrated in Figs. 3 and 4. The compressive strength (f_c) was determined from cube specimen of 150 × 150 × 150 mm^3, the split tensile strength (f_t) from cylindrical specimen of height of 300 mm and diameter of 150 mm and the flexural strength (f_r) from prismatic specimen of size of 350 × 150 × 150 mm^3.

Table 6. Strength attributes of GPC-Mixtures

Mixtures	Strength in compression (f_c), MPa	Strength obtained from split tensile test (f_t), MPa	Strength obtained after transverse loading (f_r), MPa
GPC-M_1	24.45	2.35	3.62
GPC-M_2	28.52	2.46	3.98
GPC-M_3	30.48	3.17	4.10
GPC-M_4	33.78	3.58	4.32
GPC-M_5	36.43	3.97	4.78
GPC-M_6	37.78	4.32	5.12
GPC-M_7	41.63	4.44	5.60
GPC-M_8	35.64	3.88	4.76
GPC-M_9	29.15	3.01	4.21

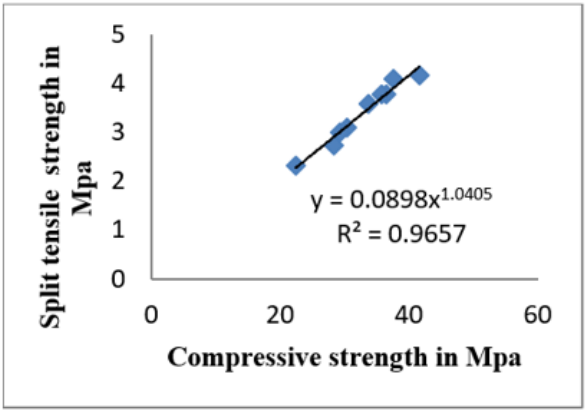

Fig. 3. Dependence strength obtained from split tensile test (f_t) on strength in compression (f_c)

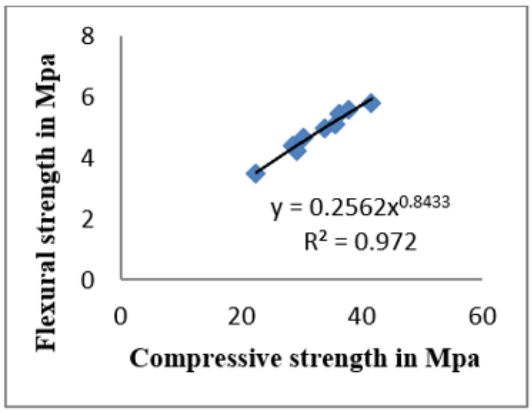

Fig. 4. Dependence strength obtained after transverse loading (f_r) on strength in compression (f_c)

The relationships between these concrete strengths were established through regression analysis, as illustrated in the equations:

$$f_t = 0.898 f_c^{1.040}, \quad (1)$$

$$f_r = 0.256 f_c^{0.843}. \quad (2)$$

The design with the largest flexural strength among the various mixtures was chosen for the production of fiber-reinforced Geopolymer concrete. The strength of fiber-reinforced concrete is influenced by various factors [33]. The selected type of fibers was added with selected mix GPC-M7 by varying volume fraction with selected aspect ratio of 60 [34]. The steel fiber added geopolymer concrete mixtures (SF-GPC-M) are depicted

in Table 7. The correlation of strength parameters f_{tf} and f_{rf} of SF-GPC-M, mixtures on fibre fraction V_f are illustrated in Figs. 5 and 6.

Table 7. Attributes of strength of SF-GPC-Mixtures

Mixtures	Fiber volume fraction (V_f), %	Compressive strength (f_{cf}), MPa	Split tensile strength (f_{tf}), MPa	Flexural strength (f_{rf}), MPa
SF – GPC - M_1	0.3	35.40	5.38	5.46
SF – GPC - M_2	0.34	33.92	5.65	5.61
SF – GPC - M_3	0.5	33.15	5.75	5.85
SF – GPC - M_4	0.8	32.54	5.15	6.06
SF – GPC - M_5	1.0	30.95	6.01	6.13
SF – GPC - M_6	1.2	30.18	5.25	6.33
SF – GPC - M_7	1.4	29.48	5.12	5.93

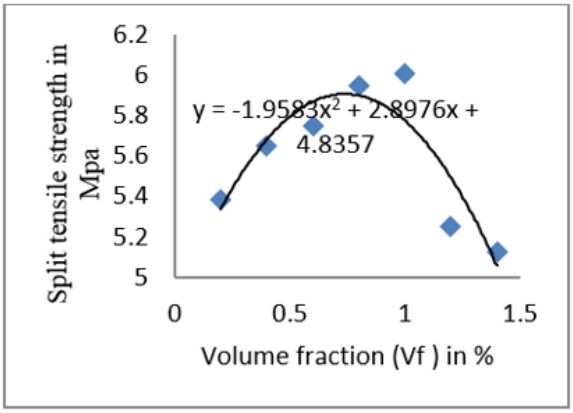

Fig. 5. Dependence split tensile strength (f_{tf}) on fiber volume fraction (V_f)

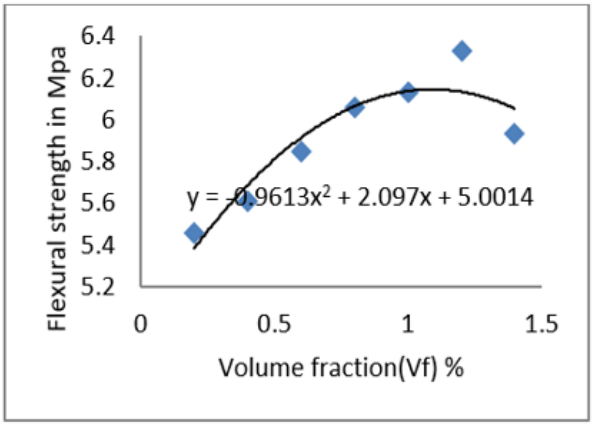

Fig. 6. Dependence flexural strength (f_{rf}) on fiber volume fraction (V_f)

The correlation of strength parameters f_{tf} and f_{rf} of SF-GPC-M mixtures on f_{cf} are illustrated in Figs. 7 and 8 respectively. The compressive strength, flexural strength and split tensile stength of SF-GPC-M mixtures over GPC-M_7 mix indicated in Figs. 9–11, respectively.

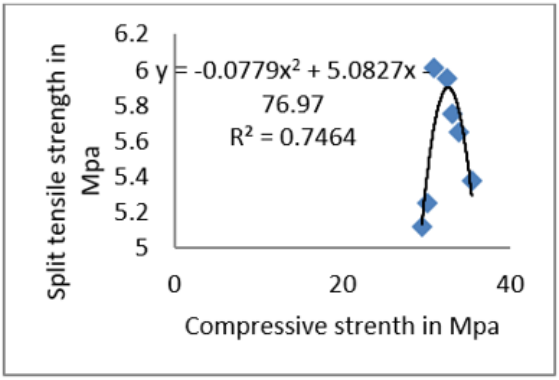

Fig. 7. Dependence split tensile strength (f_{tf}) on compressive strength (f_{cf})

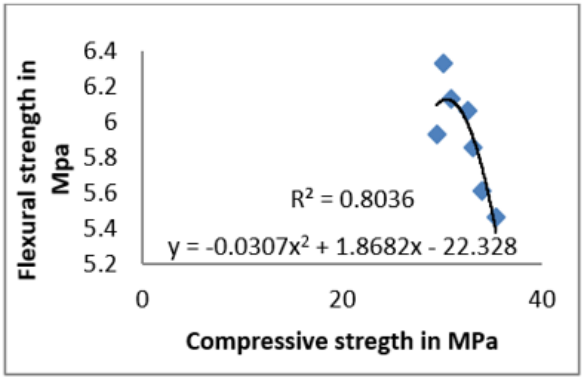

Fig. 8. Dependence flexural strength (f_{rf}) on compressive strength (f_{cf})

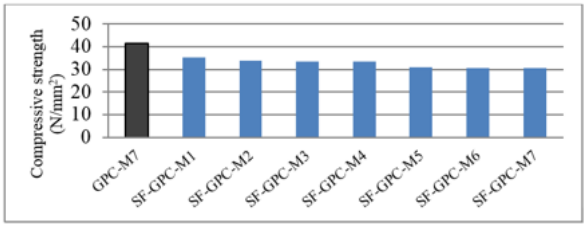

Fig. 9. Compressive strength of steel fiber-geopolymer concrete mixes over geopolymer concrete-M_7

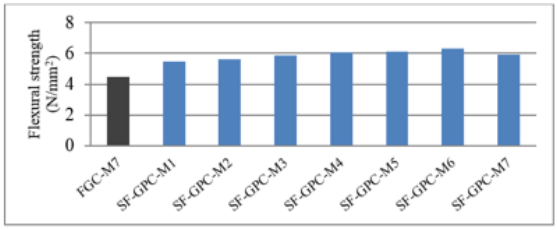

Fig. 10. Flexural strength of steel fiber-geopolymer concrete mixes over geopolymer concrete-M_7

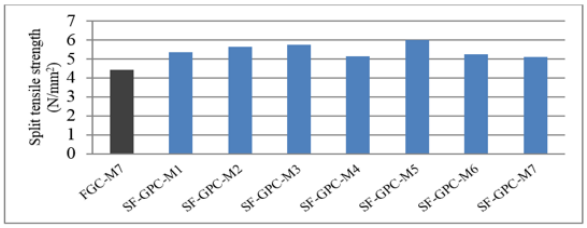

Fig. 11. Split-tensile strength of steel fiber-geopolymer concrete mixes over geopolymer concrete-M_7

Mechanical strength of steel fiber-GPC-mixtures with aspect ratio of 60 is shown in the equations:

$$f_{tf} = -1.95{V_f}^2 + 2.89V_f + 4.83, \quad (3)$$

$$f_{rf} = -0.961{V_f}^2 + 2.10V_f + 5.0, \quad (4)$$

$$f_{tf} = -0.078{f_{cf}}^2 + 5.1f_{cf} - 77.0, \quad (5)$$

$$f_{rf} = -0.030{f_{cf}}^2 + 1.86f_{cf} - 22.0\,. \quad (6)$$

Manufacturing of beams

The mix, FGC-M7 was selected due to optimum compressive strength and as well as flexural strength for manufacturing of GR-GPC and PS-GPC beams. The mix SF-GPC-M6 with volume fraction of 1.2 % was selected for SFR-GPC beam due to higher flexural strength among the mixes. All the aforesaid types of the beams were manufactured with same size. Figure 12 illustrates the dimensions of the beam and reinforcement details for Generally Reinforced-GPC and Steel Fiber Reinforced-GPC beams. The form work arrangements for beam were prepared for afore said types of beams as indicated in Fig. 13. The reinforcements were placed in the form work shown Fig. 14.

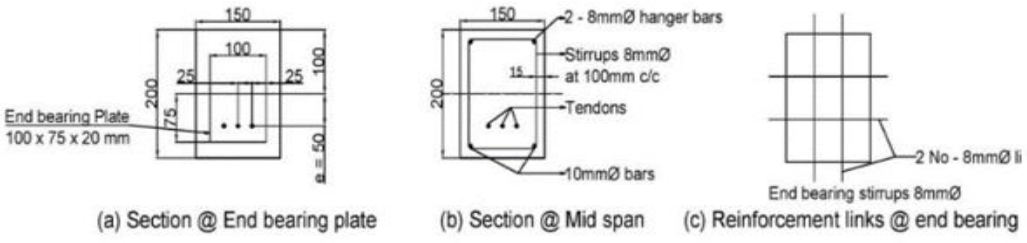

Fig. 12. GR-GPC and SFR-GPC beams reinforcement

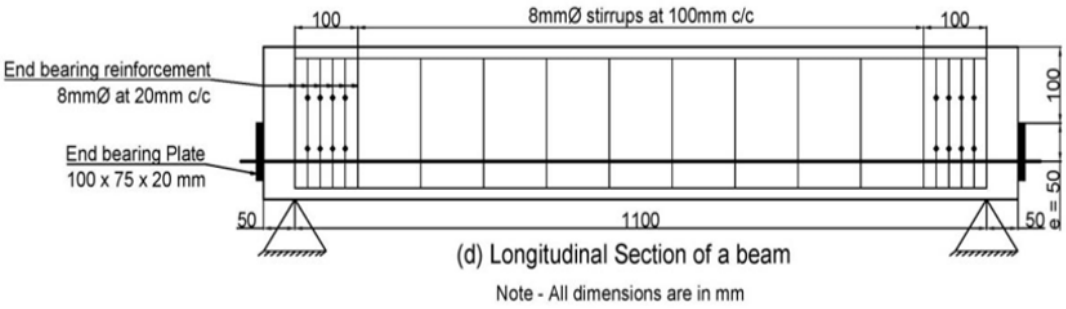

Fig. 13. Reinforcement detailing for PS-GPC beams

Fig. 14. Formwork arrangement

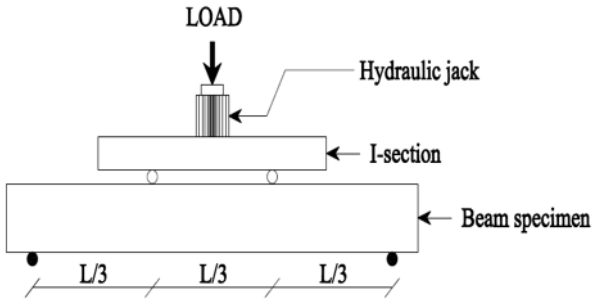

Fig. 15. Schematic of two-point loading

The concrete preparation process was conducted as detailed in the next section. Fibers were introduced into the mixer machine after blending the fine and coarse aggregates, but prior to incorporating fly ash to prepare the SF-GPC mixtures. Concrete was poured where each layer of concrete was compacted by using tamping rod. The concrete surface was leveled properly by using straight edge. A flexible PVC tube with a diameter of 10 mm was utilized as a sheathing, positioned at a specified eccentricity to accommodate the tendons. Proper care has been taken to avoid the concrete passing into the duct or sheathing of PS-GPC beams while placing and compacting the concrete in the form work. Manufactured beams were kept for three days as the rest period and temperature cured at 65 ºC for 24 h in HACC.

Post tensioning operation

The high strength steel tendons diameter of 7 mm was used to transfer the prestressing force. The barrel and wedges were used to anchor the tendons over the mild steel bearing plate. To withstand the bursting force generated during the post-tensioning process, bearing plates or end plates measuring 100 × 75 × 20 mm^3 were employed. After the temperature curing process, the beams were removed from the high alumina cement concrete (HACC), and the tendons were inserted into the duct. The prestress staple gun of 40 tonnes capacity was used to transfer the tension force in tendons. The required amount of prestress force of 35 kN is transferred to tendons and anchored with barrels and wedges. The details of top and bottom reinforcement (non-prestressed steel) are similar for all types of the beam as shown in reinforcement detail. The effect of non prestressing steel is not discussed in these investigations.

Beams testing

All beams underwent testing using the two-point loading method. The loading process is as depicted in Figs. 15 and 16. The beams were supported on a loading frame with a capacity of 50 tonnes, and the load was incrementally applied. The beam deflection was measured. Demountable mechanical gauges, with a gauge length of 200 mm and capable of measuring up to 8 microstrains, were used, as shown in Fig. 17. Cracks in the beam were marked and observed, as illustrated in Fig. 18.

Fig. 16. Test setups for beam

Fig. 17. Strain measurement at 0.42 x_u

Fig. 18. Marking of cracks

Results and Discussion

The experimental test outcomes averaged are given in Table 8. The load versus deflection at the centre of the span are presented in the graph, shown in Fig. 19. The strain measured at the depth of 0.42 x_u shown in Fig. 20. The comparison of load–deflection and load–strain responses (Figs. 19 and 20) indicates that PS-GPC consistently exhibited superior performance compared to SFR-GPC and GR-GPC. The peak load of PS-GPC was about 20–25 % higher than SFR-GPC and 35–40 % higher than GR-GPC, while SFR-GPC showed an improvement of 10–15 % over GR-GPC. In terms of deformation characteristics, PS-GPC sustained nearly 15–20 % higher deflection and 20–25 % higher strain than SFR-GPC, and 25–35 % higher deflection and 30–35 % higher strain than

Table 8. Experimental test results

Beam	Average peak load, kN	Deflection Δ_y, mm	Stiffness, kN/m	Intial crack strain	Failure load, kN	Ultimate load deflection Δ_u, mm	Failure strain	Ratio of ductility Δ_u/Δ_y
GR-GPC	47	3.25	14.46	0.010	74	10.45	0.030	3.21
SFR-GPC	55	3.08	17.85	0.009	86	10.25	0.035	3.37
PS-GPC	68.6	3.52	19.48	0.006	100	12.03	0.036	3.41

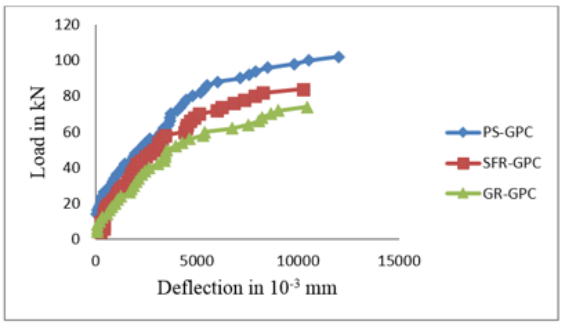

Fig. 19. Comparison of load versus deflection

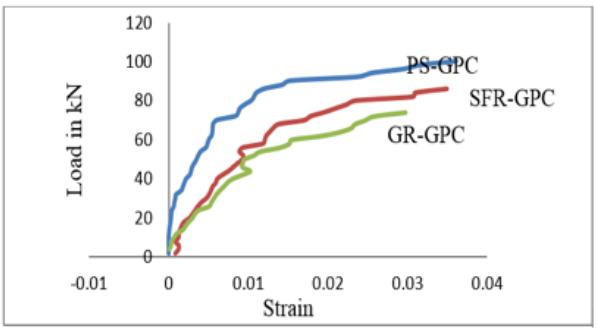

Fig. 20. Load versus strain at 0.42 x_u depth

GR-GPC. These variations clearly demonstrate that the incorporation of precipitated silica significantly enhances both load-carrying capacity and ductility of geopolymer concrete, followed by steel fiber reinforcement, whereas glass reinforcement resulted in relatively lower improvements.

The observed crack patterns (Figs. 21–23) highlight distinct modes of failure among the GR-GPC, SFR-GPC, and PS-GPC beams. In GR-GPC beams (Fig. 21), flexural cracks initiated at the tension face and propagated vertically towards the compression zone, indicating a typical brittle flexural failure with limited energy absorption. In contrast, SFR-GPC beams (Fig. 22) exhibited enhanced tenacity, as the presence of steel fibers enabled gradual dissipation of energy through multiple fine cracks. This crack-bridging effect delayed the localization of damage and improved ductility compared to GR-GPC. On the other hand, PS-GPC beams (Fig. 23) carried higher loads but developed sudden, wider cracks beyond the limiting yield stresses of the bottom layers. The failure mode in these beams was characterized by combined shear-flexural cracking, demonstrating the higher stiffness of the matrix but reduced crack control in comparison with fiber-reinforced counterparts. Overall, flexural failure dominated in GR-GPC and SFR-GPC beams, while PS-GPC beams exhibited a shear-flexural failure mode.

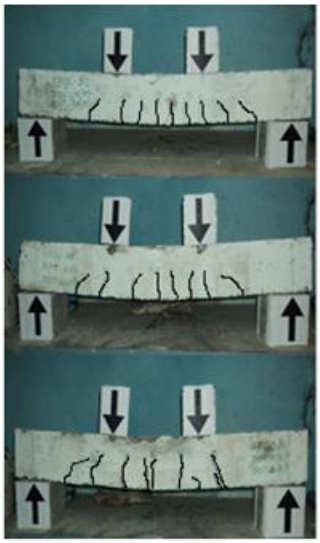

Fig. 21. Pattern of failure of GR-GPC beam

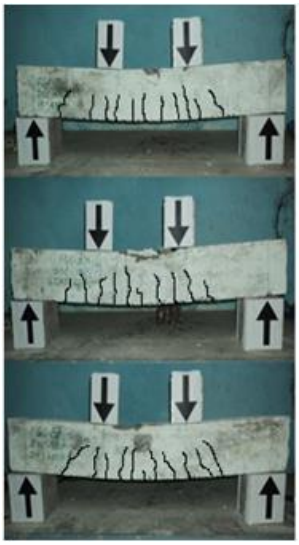

Fig. 22. Pattern of failure of SFR-GPC beams

Fig. 23. Pattern of failure of PS-GPC beams

Conclusions

Based on the experimental investigation on generally reinforced (GR-GPC), steel fiber reinforced (SFR-GPC), and pre-stressed (PS-GPC) geopolymer concrete beams, the following conclusions can be drawn:

1. SFR-GPC and PS-GPC beams achieved approximately 14 and 32 % higher peak load capacity, respectively, compared to GR-GPC beams.
2. The stiffness of SFR-GPC and PS-GPC beams was found to be 22 and 25 % higher, respectively, than that of GR-GPC beams.
3. All beam types exhibited deflections within the permissible limits specified by the Span/250 ratio under elastic conditions, up to or just before the onset of cracking.
4. At maximum load in the elastic region, SFR-GPC and PS-GPC beams recorded approximately 10 and 40 % lower strain values, respectively, than GR-GPC beams. The maximum strain values observed were 0.036 for SFR-GPC, 0.035 for PS-GPC, and 0.030 for GR-GPC beams.
5. Both SFR-GPC and PS-GPC beams demonstrated improved ductility, with ductility ratios of 6–7 % higher than GR-GPC beams.
6. GR-GPC and SFR-GPC beams exhibited predominantly flexural cracking, although SFR-GPC showed a greater number of finer cracks due to the crack-bridging action of fibers. In contrast, PS-GPC beams displayed combined shear-flexural failure, with diagonal tension cracks indicating the dominance of shear in the failure mechanism.

Overall, the study demonstrates that the incorporation of steel fibers and the use of pre-stressing significantly enhance the structural performance of geopolymer concrete beams in terms of strength, stiffness, ductility, and crack control. These findings support the application of advanced geopolymer composites in structural elements, contributing to the development of more durable and sustainable infrastructure.

CRediT authorship contribution statement

T.Q.K. Lam: writing – review & editing, writing – original draft; **K.S. Sreekeshava**: conceptualization, original draft; **S. Kumar**: supervision, investigation and conceptualization; **C. Bhargavi**: writing-review and editing, investigation; **B.N. Skanda Kumar:** visualization, testing; **G. Gayathri**: review and editing, supervision; **Y.R. Suresh**: supervision, investigation and data curation.

Conflict of interest

The authors declare that they have no conflict of interest.

References

1. Davidovits J. Geopolymers. *Journal of Thermal Analysis.* 1991;37(8): 1633–1656.
2. Lloyd N, Rangan BV. Geopolymer concrete with Fly Ash. In: Zachar J, Claisse P, Naik TR, Ganjian E. (eds.) *Proceedings of the Second International Conference on Sustainable Construction Materials and Technologies, 28–30 June 2010, Ancona, Italy.* UWM Center for By-Products Utilization; 2010. p.1493–14504.
3. Nair A, Aditya SD, Adarsh RN, Nandan M, Dharek MS, Sreedhara BM, Prashant SC, Sreekeshava KS. Additive Manufacturing of Concrete: Challenges and opportunities. *IOP Conference Series: Materials Science and Engineering.* 2020;814: 012022.

4. Nuruddin MF, Malkawi AB, Fauzi A, Mohammed BS, Al-Mattarneh HM. Geopolymer concrete for structural use: Recent findings and limitations. *IOP Conference Series: Materials Science and Engineering.* 2016;133: 012021.
5. Anilkumar S, Sreekeshava KS, Bhargavi C. Studies on Optimization of Fly Ash, GGBS and Precipitated Silica in Geopolymer Concrete. *Construction Materials.* 2025;5(2): 29.
6. Rangnath RV, Saleh M. Some optimal values in Geopolymer concrete incorporating fly ash. *Indian Concrete Journal.* 2008;82(10): 26–35.
7. Hardjito D, Rangan BV. *Development and properties of low-calcium fly ash-based Geopolymer concrete.* Faculty of Engineering Curtin University of Technology. Research Report GC 1, 2005.
8. ACI Committee 318. *Building Code Requirements for Structural Concrete and Commentary.* American Concrete Institute; 2008.
9. Comité Euro-International du Béton (CEB). *Evaluation of the Time Dependent Behaviour of Concrete.* Lausanne: CEB; 1991. Bulletin No. 199.
10. Neville AM. *Properties of Concrete.* 4th ed. Essex: Longman Group Ltd.; 1995.
11. Indian Standards. IS 456:2000. *Indian Standard Code of Practice for Plain and Reinforced Cement Concrete.* New Delhi: Bureau of Indian Standards; 2000.
12. British Standards Institution. BS 8110-1:1985. *British Standard Structural Use of Concrete: Code of Practice for Design and Construction.* London: British Standards Institution; 1985.
13. Bencardino F, Rizzuti L, Spadea G, Swamy RN. Stress-Strain Behavior of Steel Fiber-Reinforced Concrete in Compression. *Journal of Materials in Civil Engineering.* 2008;20(3): 255–263.
14. Ganesan N, Indira PV, Santhakumar A. Engineering properties of steel fibre reinforced geopolymer concrete. *Advances in Concrete Construction.* 2013;1(4): 305–318.
15. Song PS, Hwang S. Mechanical properties of high-strength steel fiber-reinforced concrete. *Construction and Building Materials.* 2004;18(9): 669–673.
16. Bernal S, de Gutierrez R, Delvasto S, Rodriguez E. Performance of Geopolymeric Concrete Reinforced with Steel Fibers. In: *Proceedings of the 10th Inorganic-Bonded Fiber Composite Conference (IIBCC 2006), 15-18 November 2006, Sao Paulo, Brazil.* New-York: Curran Associates, Inc.; 2006. p.220–232.
17. Kumar S, Rajendra S, Sreekeshava KS. Assessment of the shear strength of fly ash-based geopolymer concrete. In: Vinyas M, Loja A, Reddy KR. (eds.) *Advances in Structures, Systems and Materials. Lecture Notes on Multidisciplinary Industrial Engineering.* Singapore: Springer; 2020. p.277–286.
18. Al-Majidi MH, Lampropoulos A, Cundy AB. Steel fibre reinforced geopolymer concrete (SFRGC) with improved microstructure and enhanced fibre-matrix interfacial properties. *Construction and Building Materials.* 2017;139: 286–307.
19. Ramadoss P, Nagamani K. Investigation on the tensile strength of high-performance fiber reinforced concrete using statistical methods. *Computers and Concrete.* 2006;3(6): 389–400.
20. Mohammadi Y, Singh SP, Kaushik SK. Properties of steel fibrous concrete containing mixed fibres in fresh and hardened state. *Construction and Building Materials.* 2008;22(5): 956–965.
21. Bisht M, Iqbal MA, Kamran K, Bratov V, Morozov NF. Numerical study of thin UHPC targets response against ballistic impact. *Materials Physics and Mechanics.* 2022;50(1): 74–88.
22. Erofeev VT, Korotaev SA, Vatin NI. Deformation and Heat-Insulating Characteristics of Light Concrete on Porous Burned Binder Under Heating. *Materials Physics and Mechanics.* 2023;51(1): 33–41.
23. Xu B, Shi HS. Correlations among mechanical properties of steel fiber reinforced concrete. *Construction and Building Materials.* 2009;23(12): 3468–3474.
24. Hueste MBD, Chompreda P, Trejo D, Cline DBH, Keating PB. Mechanical properties of high-strength concrete for prestressed members. *ACI Structural Journal.* 2004;101(4): 457–465.
25. Thomas J, Ramaswamy A. Mechanical Properties of Steel Fiber-Reinforced Concrete. *Journal of Materials in Civil Engineering.* 2007;19(5): 385–392.
26. Indian Standards. IS 3812-1:2003. *Indian Standard Specification for Pulverized Fuel Ash.* New Delhi: Bureau of Indian Standards; 2003.
27. Indian Standards. IS 9103:1999. *Indian Standard Concrete Admixtures — Specification.* New Delhi: Bureau of Indian Standards; 1999.
28. Bhargavi C, Sreekeshava KS, Sunagar P, Dharek MS, Ganesh CR. Mechanical Properties of Steel and PolypropyleneFiber Reinforced Geopolymer Concrete. *Journal of Mines, Metals and Fuels.* 2023;71(7): 984–989.
29. Hardjito D, Wallah SE, Sumajouw DMJ, Rangan BV. On the development of fly ash-based geopolymer concrete. *ACI Materials Journal.* 2004;101: 467–472.

30. Pradeepa J, Kumar S, Ravindra PM. Cost-effective curing arrangement for geopolymer concrete specimens. *International Journal of Emerging trends in Engineering and Development.* 2012;2(7): 227–233.
31. van Jaarsveld JGS, van Deventer JSJ, Lukey GC. The effect of composition and temperature on the properties of fly ash and kaolinite-based Geopolymers. *Chemical Engineering Journal.* 2002;89(1-3): 63–73.
32. Karunanithi S, Anandan S. Flexural Toughness Properties of Reinforced Steel Fibre Incorporated Alkali Activated Slag Concrete. *Advances in Civil Engineering.* 2014; 2014(1): 719436.
33 Li Z, Zhang Y, Zhou X. Short Fiber Reinforced Geopolymer Composites Manufactured by Extrusion. *Journal of Materials in Civil Engineering.* 2005;17(6): 624–631.
34. Kumar S, Pradeepa J, Ravindra PM, Rajenda S. Experimental approach to study the properties of fiber reinforced fly ash based geopolymer concrete. *International Journal of Informative & Futuristic Research.* 2015;2(8): 2625–2635.